

# Fluorescence Study of Field-Induced Director Reorientations in Low Mass Liquid Crystalline Compounds

J. Hofkens,<sup>1</sup> M. Van Damme,<sup>1</sup> F. C. De Schryver,<sup>1</sup> and T. G. Ryan<sup>2</sup>

Received February 4, 1991; revised September 13, 1991; accepted September 24, 1991

The Frederickz transition and the dynamic scattering deformation in 4-alkyloxy-4'-cyanobiphenyl compounds are investigated by fluorescence spectroscopy and turbidimetry. The main characteristics of the Frederickz deformation, reversibility and threshold voltage, in the nematic and the smectic A phase are investigated by means of fluorescence spectroscopy. Furthermore, the dynamics of the Frederickz transition are studied as a function of temperature and applied voltage. The results obtained with both techniques are compared and correlate well.

**KEY WORDS:** Frederickz transition; fluorescence; turbidimetry; 4-alkyloxy-4'-cyanobiphenyl; liquid crystals.

## INTRODUCTION

In an electric field low molecular weight liquid crystals can undergo different director reorientations, e.g., the Frederickz transition, the DAP effect (distortion of an aligned phase), the formation of William's domains, and the dynamic scattering [1]. One of the main deformations known for liquid crystals is the Frederickz transition [2]. Upon applying a high-frequency electric field the mesogens tend to align themselves with their director parallel to the field ( $\Delta\epsilon > 0$ ), resulting in a homeotropic orientation (Fig. 1). Up to now the dynamics of this reorientation have been investigated through electrooptical measurements under the polarization microscope [3-9]. To detect the changing light intensity through the sample upon applying an electric field, a photodiode is used and the signal is transferred to a recorder or an oscilloscope [10]. The threshold voltage  $V_d$  [Eq. (1)] and

<sup>1</sup> Department of Chemistry, Katholieke Universiteit Leuven, Celestijnenlaan 200F, B-3001 Heverlee, Belgium.

<sup>2</sup> ICI, Wilton Materials Research Centre, P.O. Box 90, Wilton Middlesbrough, Cleveland TS6 8JE, England.

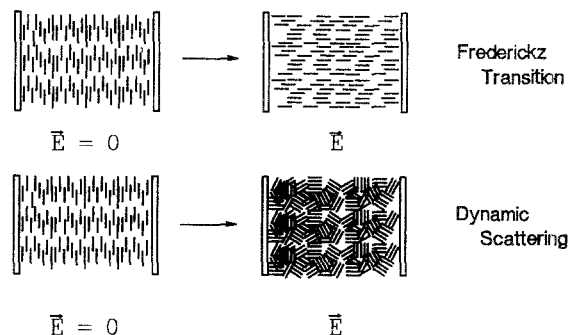


Fig. 1. Representation of the reorientation that occurs at the Frederickz transition and dynamic scattering.

the response time  $\tau_r$  [Eq. (2)] are the two main properties which characterize the Frederickz transition. The initial orientation in the sample cell (the director is aligned parallel to the glass plates) is deformed by an electric field if the applied voltage  $V$  is larger than the threshold voltage  $V_d$  [Eq. (1)].

$$V_d = \pi(k_{11}/\epsilon_0 \Delta\epsilon)^{1/2} \quad (1)$$

If such a voltage is applied, the deformation to the new equilibrium state requires time. This response time  $\tau_r$  depends on characteristic material parameters [Eq. (2)].

$$\tau_r = \frac{\eta d^2}{\epsilon_0 \Delta\epsilon V^2 k_{11} \pi^2} \quad (2)$$

In this equation  $k_{11}$  is the elastic constant for splay,  $\Delta\epsilon$  is the dielectric anisotropy,  $\eta$  is the viscosity of the sample,  $d$  is the thickness, and  $V$  is the applied voltage. Using a low-frequency AC electric field, the clear liquid crystalline state is converted to a turbulent light-scattering state. The scattering state consists of small scattering centers which, in the driven mode, are in a continuous stage of agitation (Fig. 1).

The photophysical properties of 4-alkyl- and 4-alkoxy-4'-cyanobiphenyl compounds in the neat phases have been reported previously [11-18]. As a consequence of the specific photophysical properties of each phase, it is possible to determine the phase transition temperatures by monitoring the fluorescence intensity as a function of the temperature [11,13,14,16,17,19,20]. The discontinuities in the relative intensity correspond to the phase transition temperatures. A first basis for these discontinuities upon a phase change is therefore related to the change in photophysical properties of the phases. The emission in the crystalline state is due mainly to monomer emission, while in the liquid crystalline state and the isotropic state both monomer- and excimer-type emissions are observed. The different properties of these excited states cause discontinuities in the fluorescence intensity at the phase transition. Furthermore, the differences in refractive index and rigidity also contribute to different fluorescence intensities and therefore to discontinuities at the phase transitions.

In this paper the phase transition is also studied by means of turbidimetry. It was shown that results received by both techniques do agree well. The aim of this work is to show that both fluorescence and turbidimetry can be used to investigate electric field induced reorganizations in liquid crystals as a function of temperature, time, and voltage. From this point of view the reversibility and the threshold voltage of the Fredericksz transition in the nematic and the smectic liquid crystalline state of 4-cyano-4'-alkoxybiphenyl compounds, as well as the dynamics of this transition as a function of temperature and applied field, were studied. Furthermore, the dynamic scattering of those liquid crystals, due to a low-frequency electric field, was examined.

## EXPERIMENTAL

The liquid crystalline samples were prepared between transparent, electrically conducting In/SnO<sub>2</sub>-coated glass plates (GLAVERBEL) separated by a spacing epoxy glue to give electrode separations of 20  $\mu$ m. The thickness was determined by absorption measurements. For applying AC voltage of variable frequency, a HAMEG function generator HM8030-2 in combination with a self-made amplifier was used. This combination produced AC square waves up to 120 V<sub>eff</sub> in a frequency range of 30 Hz to 20 kHz. The applied voltage was checked by a multimeter.

The phase transitions and the electric field-induced reorientations were monitored by microscope examination (Nikon Optiphot) between crossed polarizers using a microfurnace (Mettler FP82). The turbidimetric measurements were recorded on a PERKIN ELMER lambda 6 spectrophotometer ( $\lambda_{AN}$ , 700 nm). The fluorescence spectra were taken under thermostated conditions (using the Mettler FP82 hot stage) on a Spex fluorolog. The liquid crystals used in the present study were 4-butoxy-4'-cyanobiphenyl (4COB), 4-octyloxy-4'-cyanobiphenyl (8COB), 4-nonyloxy-4'-cyanobiphenyl (9COB), and 4-dodecyloxy-4'-cyanobiphenyl (12COB), obtained from BDH. They were shown to be free from impurities by HPLC. These products undergo a sequence of phase transitions shown below.

	40°C	77°C	
4COB:	K → N	→ I	
	54.5°C	67°C	80°C
8COB:	K → S <sub>A</sub>	→ N → I	
	64°C	77.5°C	80°C
9COB:	K → S <sub>A</sub>	→ N → I	
	70°C	90°C	
12COB:	K → S <sub>A</sub>	→ I	

Time-resolved decay measurements were obtained with single-photon timing equipment using a synchronously pumped, cavity-dumped dye laser as excitation source [24]. A global iterative reweighted deconvolution program based on the nonlinear least-squares algorithm of Marquardt [25] was used to estimate the unknown parameters  $\alpha_j$  and  $\tau_j$ . The entire decay profiles, including the rising edge, were analyzed. Fluorescence decay curves at different wavelengths and time increments were analyzed simultaneously according to Eq. (3); the sample and reference decay time parameters (fluorescence response function of detection system about 80 ps) were linked.

$$\begin{cases} f_1 = \sum_j \alpha_j^1 \exp(-t/\tau_j) \\ f_2 = \sum_j \alpha_j^2 \exp(-t/\tau_j) \\ f_3 = \sum_j \alpha_j^3 \exp(-t/\tau_j) \\ f_i = \sum_j \alpha_j^i \exp(-t/\tau_j) \end{cases}$$

## RESULTS AND DISCUSSION

### Determination of the Phase Transition Temperature

One method to study the phase transition is turbidimetry, where transmittance, reflecting the opacity of the sample, is measured through the sample. The results of these measurements are complementary to light scattering. As a reference the transmittance of the sample in the isotropic phase is calibrated as 100%. In Fig. 2 the transmittance curves of 9COB are shown as a function of temperature.

At the temperature of the phase transition discontinuities in the transmittance are observed. The changes that occur at  $T_{NI}$  (transition temperature nematic  $\rightarrow$  isotropic) are rather small ( $Tr_I = 100\%$  and  $Tr_N = 90\%$ ), but nevertheless they are sharply defined. Only 10% of the incident light is lost by light scattering. In the crystalline phase, however, the transmittance is very small (for 9COB,  $Tr_K < 20\%$ ) due to efficient light scattering.

Different transmittance values are obtained for the  $S_A$  phase upon heating or cooling. Upon heating  $Tr_{SA} = 50\%$ , during the cooling cycle a transmittance value of 70% is obtained. Consequently a higher transparency is obtained as the  $S_A$  phase is formed by cooling the I phase. The difference in transparency is caused by the tendency of the mesogenic groups to form a homeotropic order upon cooling the I phase. If a perfect homeotropic order is adopted, the light falls in through the optical axis and there is no birefringence. In this situation the sample is totally transparent. During the cooling cycle the order in the  $S_A$  phase resembles more closely a homeotropic orientation, resulting in a higher transmittance.

### The Frederickz Transition

The influence of the reorientation, induced by the Frederickz deformation, was examined in the different phases of 4COB, 8COB, and 12COB.

In the crystalline phase the fluorescence spectrum of 4COB undergoes no changes in intensity or in shape on application of an electric field (AC  $f = 1.5$  kHz),

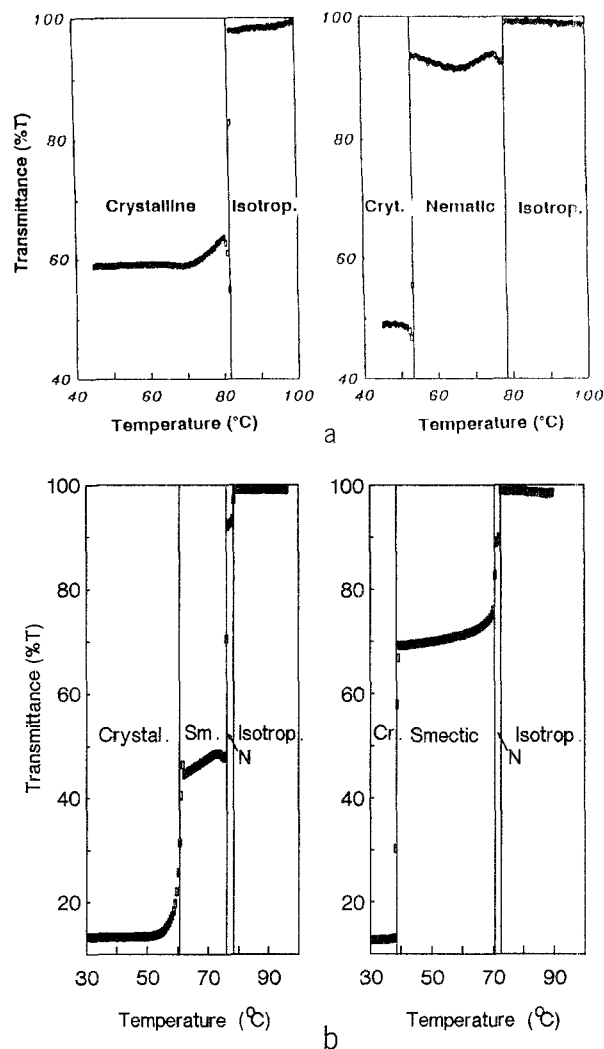


Fig. 2. (a) Transmittance ( $\lambda_{AN} = 700$  nm) of 4COB as a function of the temperature (left, heating; right, cooling cycle). (b) Transmittance ( $\lambda_{AN} = 700$  nm) of 9COB as a function of the temperature (left, heating; right, cooling cycle).

even when the applied voltage amounts to 100  $V_{eff}$ . Although the crystalline phase exhibits dielectric anisotropic properties, no reorientation is observed due to the lack of mobility in this phase.

In the isotropic phase of 4COB (90°C) a small decrease in the fluorescence intensity is observed. This decrease is due to the existence of ordered structures (100 to 150 molecules) above the clearing temperature [18,21–23]. In the presence of an electric field these locally ordered structures will undergo a reorientation which leads to a small intensity decrease.

On application of an electric AC field in the nematic

phase of 4COB (Fig. 3), the intensity of the fluorescence spectrum decreases. The shape of the spectrum, however, remains the same. The decrease in intensity is more pronounced as the applied voltage is raised.

Since the time-resolved emission properties are very sensitive to changes in the local structure, the fluorescence decay of 4COB in the nematic phase (60°C) in the absence or the presence of an electric field was globally analyzed. A three-exponential global analysis yielded good statistical parameters. Furthermore, identical parameters were obtained irrespective of the applied field (Table I), indicating that the local order remains unchanged upon applying an electric field. The globally analyzed decay parameters are in good agreement with the decay parameters obtained in a concentration study of 4COB in benzene. Assuming irreversible formation of each state, the short decay time of 150 ps could be associated with the emission from a locally excited state. The intermediate

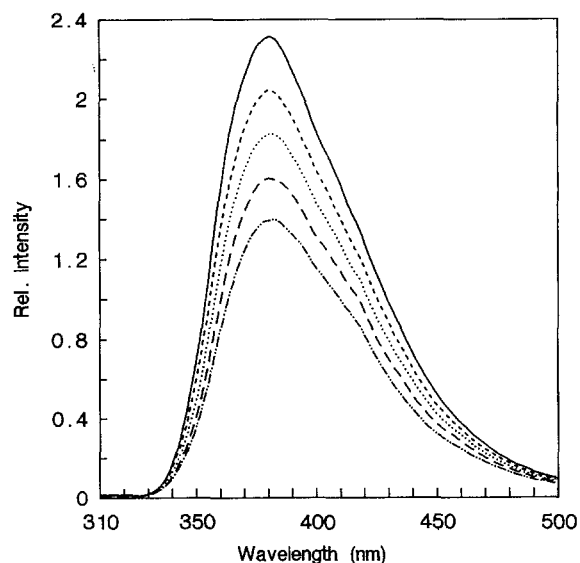


**Fig. 3.** Fluorescence spectra of 4COB (60°C) in the nematic phase (cell thickness, 20  $\mu\text{m}$ ) as a function of the applied voltage: 0  $V_{\text{eff}}$  (—); 3.7  $V_{\text{eff}}$  (-----); 7.5  $V_{\text{eff}}$  (·····); 16  $V_{\text{eff}}$  (- - - -); 106  $V_{\text{eff}}$  (-.-.-.-).

decay time (2–3 ns) could correspond to emission from an ICT state (intramolecular charge transfer state) and the long decay time (10 ns) could be due to emission from an intermolecular excited state complex. Klock and Rettig found similar results in their study of 4-alkyl-4'-cyanobiphenyl compounds [27]. A more extended discussion of the results is the subject of a forthcoming paper [28].

Smectic A phases can also be oriented in an AC electric field; however, due to the layered structure, higher field strengths are required to induce the Fredericksz deformation. On application of a high-frequency AC electric field, 1.5 kHz, the relative intensity of the emission spectrum of 12COB in the  $S_A$  phase (85°C) decreases (Fig. 4). As in the nematic phase the shape of the spectrum remains unchanged.

In Fig. 5 the electric field effect in the various phases of 8COB is displayed. From this figure it is clear that the reorientations only occur in the liquid crystalline phases. In the isotropic phase an identical intensity change is observed as for 4COB. The intensity of the crystalline phase is different according to the orientation of the phase from which it is crystallized. Crystallization from a homeotropic  $S_A$  phase yields a lower fluorescence intensity than the emission intensity from the crystalline phase which is crystallized in the absence of an electric field. Furthermore, one can observe that the stability of the  $S_A$  phase decreases on application of an electric field. The transition temperature  $T_{\text{SK}}$  [transition temperature smectic  $\rightarrow$  crystalline goes from 44°C ( $\vec{E} = 0$ ) to 34°C (AC  $f = 1.5$  kHz 90  $V_{\text{eff}}$ )].

The intensity decrease that occurs upon applying an AC electric field can be explained on the basis of the model description represented in Fig. 6. In this figure the relative orientation of the mesogens to the plane of polarization of the excitation light is schematically drawn for the different situations. The decrease in intensity originates from a decreased number of excited mesogenic groups. The experimental setup is built in such a way that at  $\vec{E} = 0$  for absorption, the transition dipoles of the mesogenic groups lie in the plane of polarization of the excitation light. As the electric field is switched

**Table I.** Decay Parameters of the Global Analysis of 4COB (Nematic Phase) in the Absence or in the Presence of an AC Electric Field (1 kHz)<sup>a</sup>

$U$	$\alpha_1$	$\tau_1$ (ps)	$\alpha_2$	$\tau_2$ (ns)	$\alpha_3$	$\tau_3$ (ns)
0 $V_{\text{eff}}$	$1.44 \pm 0.04$	$149 \pm 15$	$0.14 \pm 0.01$	$2.33 \pm 0.09$	$0.37 \pm 0.01$	$10.32 \pm 0.04$
40 $V_{\text{eff}}$	$1.57 \pm 0.04$	$149 \pm 15$	$0.18 \pm 0.01$	$2.33 \pm 0.09$	$0.37 \pm 0.01$	$10.33 \pm 0.04$

<sup>a</sup>  $Z(\chi^2)_{\text{glob}} = 1.445$  ( $\lambda_{\text{EM}} = 380$  nm,  $\lambda_{\text{EX}} = 295$  nm).

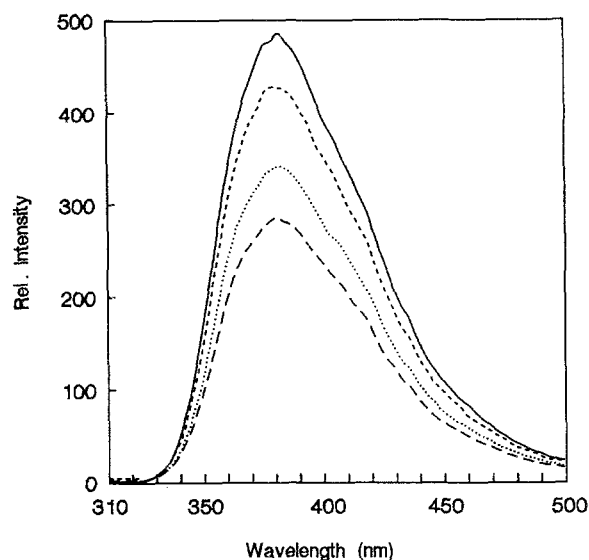


Fig. 4. Fluorescence spectra of 12COB in the  $S_A$  phase ( $85^\circ\text{C}$ ) (cell thickness  $\approx 20 \mu\text{m}$ ) as a function of the applied electric field:  $0 V_{\text{eff}}$  (—);  $50 V_{\text{eff}}$  (-----);  $55 V_{\text{eff}}$  (.....) and  $110 V_{\text{eff}}$  (- - - -).

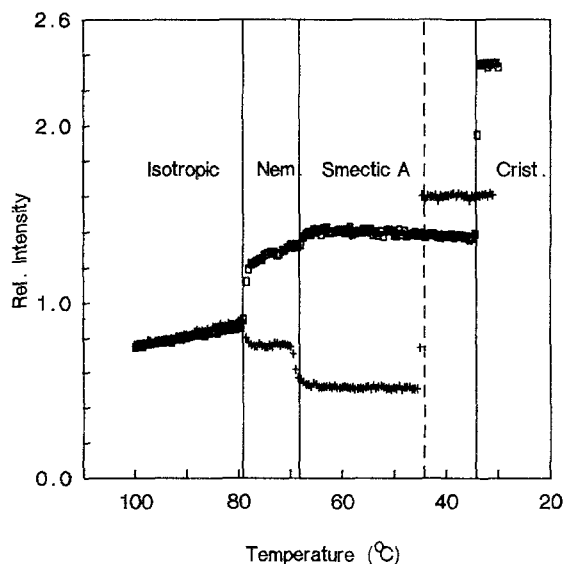


Fig. 5. Fluorescence intensity ( $\lambda_{\text{EM}} = 380 \text{ nm}$ ) of 8COB (cell thickness  $\approx 20 \mu\text{m}$ ) measured with decreasing temperature:  $\vec{E} = 0$  ( $\square$ );  $AC f = 1.5 \text{ kHz}$ ,  $90 V_{\text{eff}}$  (+).

on, the mesogenic groups tend to align parallel to the field ( $\Delta\epsilon > 0$ ). In this configuration the transition dipole of absorption is perpendicular to the plane of polarization of the excitation light. The decreased number of excited mesogens results in a decrease in emission intensity.

If a perfect homeotropic alignment is achieved, the mesogens should no longer absorb light. However, from Figs. 2 and 3 one can observe that the intensity does not drop to zero. The reason for this background fluorescence is the incomplete homeotropic ordering at the electrodes. In Fig. 7 the orientation of the mesogens at the cell surfaces in the presence of an AC electric field (Frederickz deformation) is given. At the cell surface little or no orientation is achieved. As a consequence these molecules will absorb light and are responsible for the background fluorescence which is detected even at high electric fields.

### Reversibility of the Frederickz Transition

The reversibility of the Frederickz transition was investigated in the nematic phase of 4COB ( $60^\circ\text{C}$ ) and the smectic phase of 12COB ( $85^\circ\text{C}$ ). If the deformation is a completely reversible process, the initial emission intensity should be regained upon switching off the applied electric field.

On applying an AC electric field in the nematic phase as reported in Fig. 8a, 1, a decrease in intensity is observed. As the field is switched off (Fig. 8a), the initial intensity is restored within 25 ms.

In the  $S_A$  phase of 12COB an identical intensity decrease is observed on application of an electric field (Fig. 8b, 1). Switching off the electric field, indicated by 2 in Fig. 8b, however, does not lead to an increase in the intensity. This nonreversible behavior is the basis for thermo- and laser addressing applications of smectic A phases.

In an electrooptic cell the deformation is introduced through the effect of the external electric field on the dielectric properties. The reorientation is the result of elastic forces. Compared to the solid state, the elastic forces in liquid crystalline phases are very weak. In the nematic phase the elastic forces are strong enough to induce a reorientation, while in the  $S_A$  phase the elastic forces are too weak to reinduce the initial orientation.

### Determination of the Threshold Voltage

The Frederickz transition is characterized by a threshold voltage. The threshold voltage is the minimum voltage required to pull the director out of its original position. In Fig. 9 the fluorescence intensity of 4COB in the nematic phase as a function of the applied voltage ( $AC f = 1 \text{ kHz}$ ) is given. The inset shows a magnification of the first part of the curve. The intensity starts to drop from a certain threshold voltage  $V_d$ . This is observed in the nematic phase of 4COB ( $60^\circ\text{C}$ ) at a thresh-

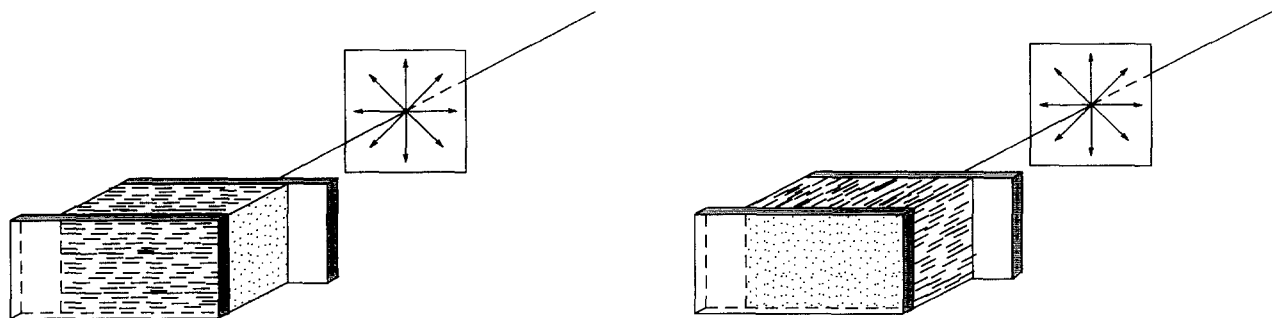


Fig. 6. Schematic drawing of the orientation of the mesogenic groups with respect to the plane of polarization of the excitation light (left, homogeneous orientation; right, homeotropic orientation).

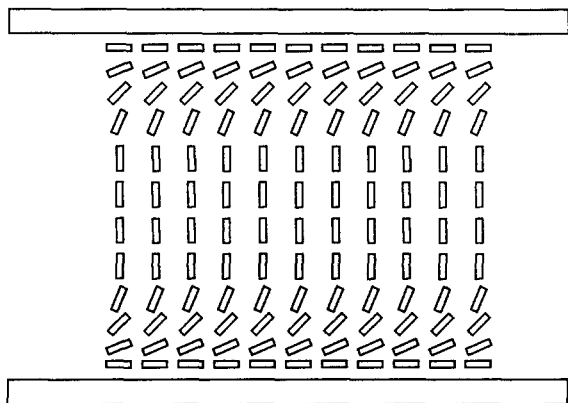


Fig. 7. Schematic drawing of the orientation of the mesogenic groups at the electrode. At the electrode surfaces the mesogenic groups possess a homogeneous orientation. With increasing distance from the electrode, a homeotropic orientation is induced.

old voltage of  $1.1 V_{\text{eff}}$ . In the range of 0 to  $20 V_{\text{eff}}$  a strong drop in emission intensity is observed. In this range the biggest changes in orientation of the director occur. Larger fields will lead to only small changes in the director orientation. In the same way, the threshold voltage of 12COB in the  $S_A$  phase was determined:  $V_d = 17.1 V_{\text{eff}}$ .

#### Determination of the Response Time

Another quantity which characterizes the Fredericksz deformation is the response time. By monitoring the fluorescence decrease as a function of time on application of an AC electric field, it is possible to determine the response time. In this contribution the response time is defined as the time to realize 50% of the total fluorescence intensity decrease.

To determine the response time in the nematic phase of 4COB ( $60^\circ\text{C}$ ), a square voltage (AC  $f = 10 \text{ Hz}$ ,  $\tau_{\text{rise}} = 70 \text{ ns}$ ) was applied. The offset was adjusted to attain a periodically switching voltage between 0 and 15 V. The fluorescence intensity was monitored every millisecond. As shown in Fig. 10a reversible intensity changes are observed which correspond well to the changes in the applied voltage. The response time was determined from Fig. 10b, which is a magnification of one reorientation. Within 2 ms the intensity drops to half of its initial emission intensity. Reorientation to the original situation takes place on the same time scale.

The influence of the temperature on the response time of 4COB in the nematic phase was also investigated. In the temperature range of  $40 \rightarrow 60^\circ\text{C}$  very short response times ( $< 3 \text{ ms}$ ) are observed which are independent of the temperature. Since the response time changes proportionally with the viscosity, longer response times are observed for the smectic A phase compared to the nematic phase. The response time then becomes within the detection limit of the spectrophotometer (100 ms) and, therefore, can be measured with the turbidity technique. In the turbidity experiments the transmittance is monitored as a function of the time upon application of an AC electric field. At  $\vec{E} = 0$  the transmittance in the  $S_A$  phase amounts to 65%. On application of a high-frequency AC electric field (3 kHz), a homeotropic orientation is achieved and the transmittance reaches 100%. Shortly after application of the electric field a small decrease in transmittance is observed (Fig. 11b). The Fredericksz transition of the smectic phase is a complex deformation in which a layered structure is transformed into a homeotropic layered structure. Initially the layered structure is disorganized, resulting in increased light scattering. As the homeotropic orientation is achieved, the transmittance increases to 100%.

In this work the time required to realize half of the

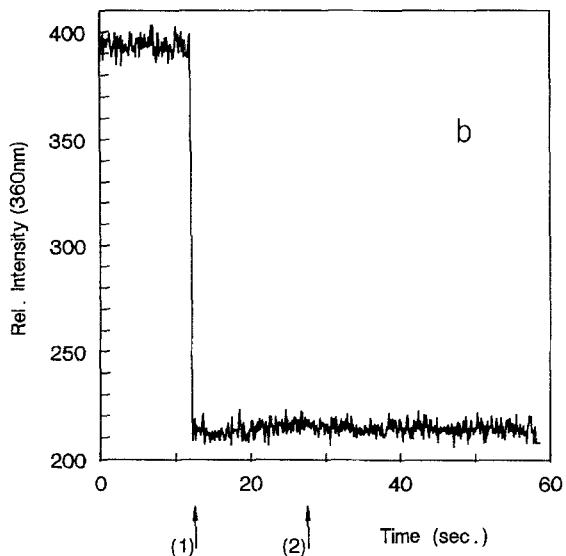
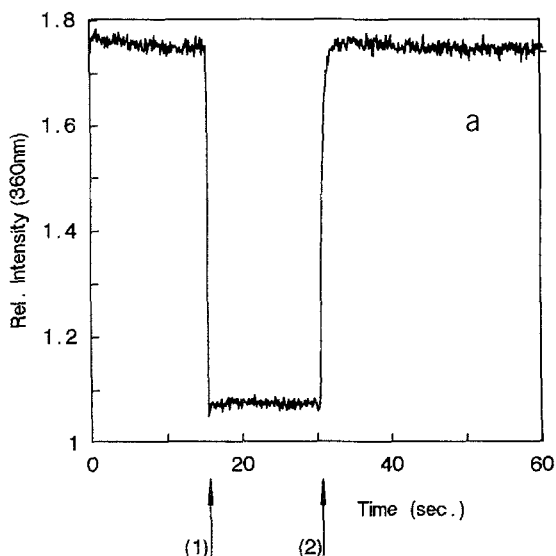


**Fig. 8.** (a) Fluorescence intensity of 4COB in the N phase (60°C) on application (1) and switching off (2) of the electric field (AC  $f = 1$  kHz,  $90 V_{eff}$ ; cell thickness  $\approx 20 \mu\text{m}$ ). (b) Fluorescence intensity of 12COB in the  $S_A$  phase (85°C) on application (1) and switching off (2) of the electric field (AC  $f = 1.5$  kHz,  $90 V_{eff}$ ; cell thickness  $\approx 20 \mu\text{m}$ ).

total transmittance increase is defined as the response time. Although the experimental noise in the fluorescence experiments (Fig. 11b) is larger than in the turbidity experiments, both techniques allow accurate determination of the response time. With both methods the influences of the temperature and the applied field were investigated. The results are displayed in Figs. 12a and b. The response times obtained with both techniques

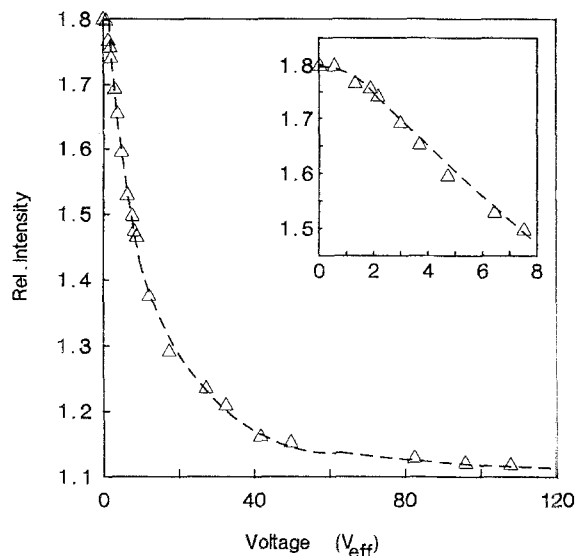


**Fig. 9.** Fluorescence intensity of 4COB in the N phase (60°C) as a function of the applied voltage (AC  $f = 1$  kHz; cell thickness  $\approx 20 \mu\text{m}$ ).

[response time obtained through fluorescence ( $\Delta$ ) and transmittance ( $\circ$ )] show a good correlation.

At a constant electric field the response time increases with decreasing temperature. The increase in viscosity is responsible for this increase. The logarithm of the response time shows a linear relationship with the inverse of the temperature. From the slope of the Arrhenius plot the activation energy of the Fredericksz transition is determined. For the  $S_A$  phase of 12COB  $E_{FT} = 352$  kJ/mol.

With decreasing field strengths larger response times are obtained. In agreement with Eq. (2), a linear relationship was found between the response time and the square of the applied voltage. On application of an AC low-frequency electric field (100 Hz) on a  $S_A$  phase which possesses a small electric resistivity ( $< 1 \times 10^9 \Omega\text{-cm}$ ), a scatter texture can be induced. This scatter texture consists of small microdomains which move turbulently. In Fig. 1 the dynamic scattering is schematically drawn. By means of turbidimetry and fluorescence, the properties of the dynamic scattering are examined. The Fredericksz deformation leads to a decrease in fluorescence intensity (Fig. 13). The dynamic scattering, however, induces an emission increase. The shape of the fluorescence spectrum remains unchanged.

In Fig. 14 the fluorescence intensity changes associated with the Fredericksz deformation and the dynamic scattering as a function of the temperature are displayed. At  $\vec{E} = 0$  (—) a small intensity decrease

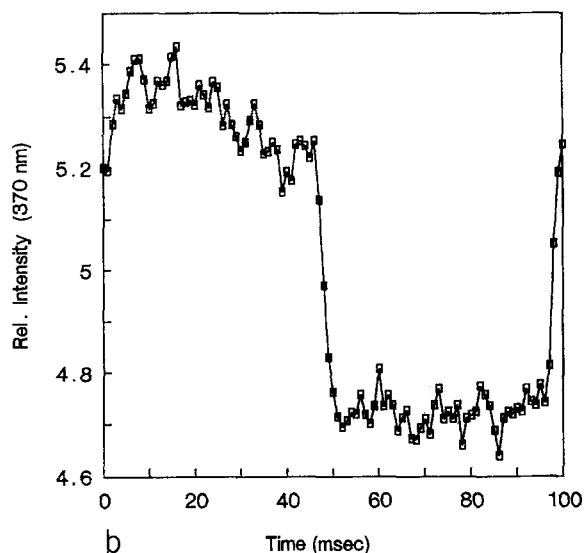
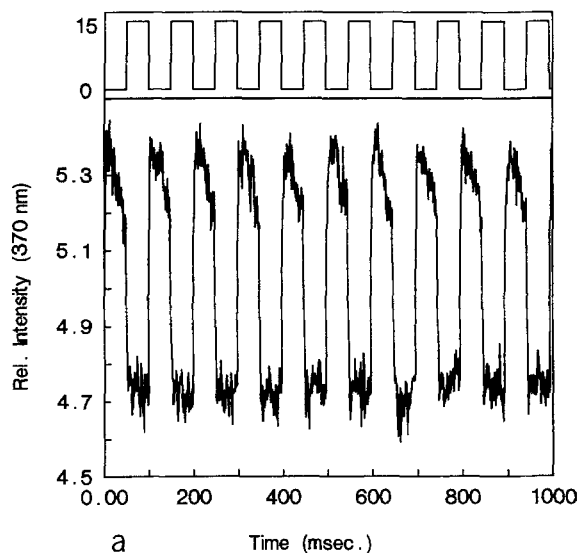


Fig. 10. (a) Fluorescence intensity of 4COB in the N phase ( $60^{\circ}\text{C}$ ) as a function of time. At the top of the figure the applied square wave is shown ( $AC f = 10 \text{ Hz}$ ). (b) Magnification from Fig. 7.15a:  $\tau_r = 2 \text{ ms}$ .

at  $T_{ISA}$  (transition temperature isotropic  $\rightarrow$  smectic A) is observed due to the tendency of the mesogens to adopt a homeotropic alignment. The decrease in intensity introduced through the Fredericksz transition is larger due to the perfect homeotropic alignment. The fluorescence intensity behavior of the dynamic scattering (low-frequency electric field; - - -) is understood as follows. Up to  $10^{\circ}\text{C}$  below  $T_{IS}$  (transition temperature isotropic  $\rightarrow$  smectic), an increase intensity is observed. In the dynamic scattering mode the microdomains are in a con-

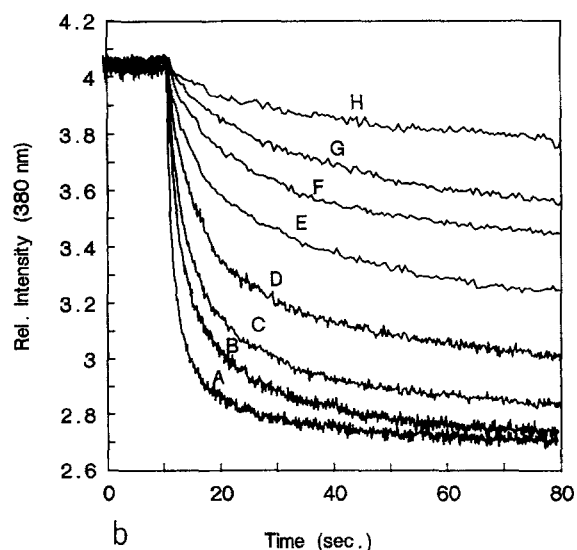
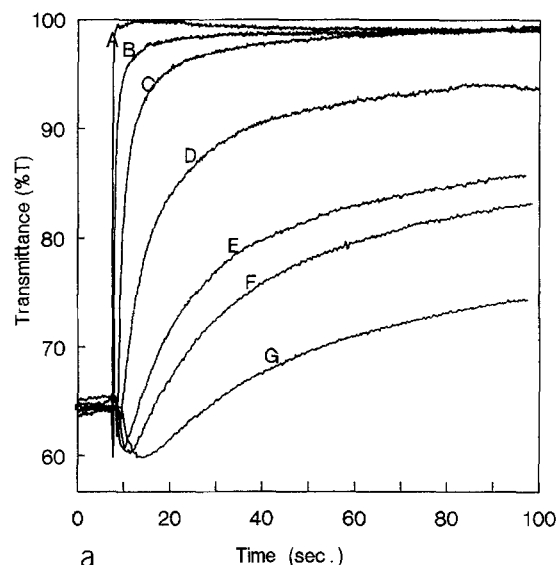


Fig. 11. (a) Transmittance ( $\lambda = 700 \text{ nm}$ ) of 12COB in the  $S_A$  phase ( $78^{\circ}\text{C}$ ) as a function of time, measured at decreasing voltages ( $AC f = 3 \text{ kHz}$ ; from a to g, decreasing voltages). (b) Fluorescence intensity ( $\lambda_{EM} = 370 \text{ nm}$ ) of 12COB in the  $S_A$  phase as a function of time, measured at decreasing temperatures (from a to g, decreasing temperatures).

stant turbulent agitation. The average number of excited mesogens will be larger than in the normal  $S_A$  ( $\vec{E} = 0$ ) phase. As the temperature decreases in the  $S_A$  phase, the turbulent nature of the dynamic scattering decreases, finally resulting in a homeotropic orientation. As a consequence the number of excited mesogens decreases with decreasing temperature, leading to a decrease in emission intensity.

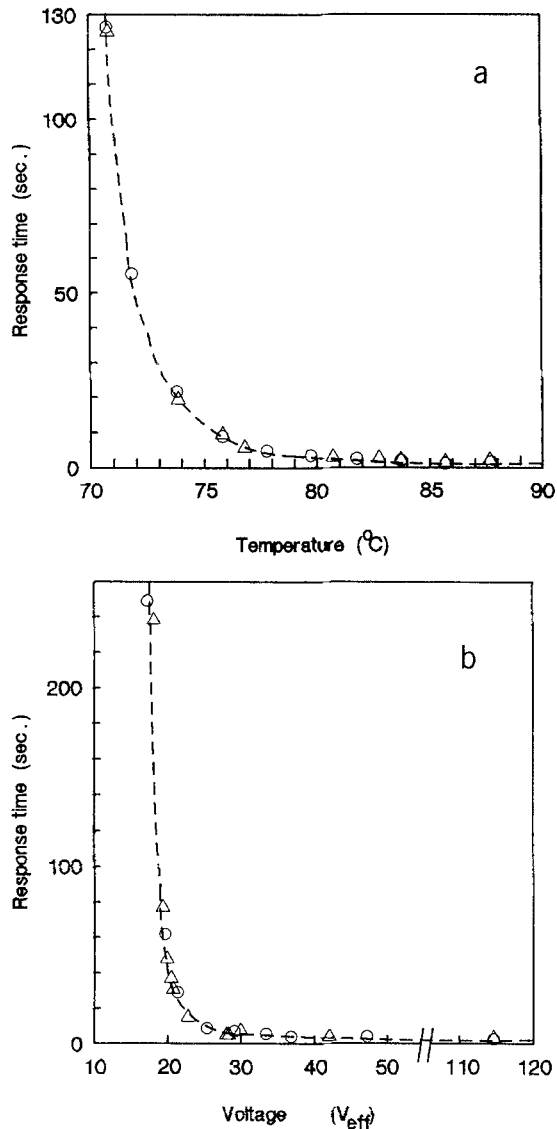


Fig. 12. (a) Response time of 12COB in the  $S_A$  phase as a function of temperature. The applied voltage was  $30 V_{eff}$  at 3 kHz; the cell thickness was  $\approx 20 \mu\text{m}$ . (b) Response time of 12COB in the  $S_A$  phase as a function of the applied voltage ( $T = 78^\circ\text{C}$ ,  $d \approx 20 \mu\text{m}$ ,  $f = 1 \text{ kHz}$ ).

The effects of the electric field deformations (Fredrickz transition and dynamic scattering) on the transmittance properties as a function of the temperature are displayed in Fig. 15. Upon applying a high-frequency AC electric field (.....) a homeotropic orientation is introduced in the  $S_A$  phase, resulting in a transmittance of 100%. As for the fluorescence measurements, the transmittance behavior on application of a low-frequency AC electric field (- - -) displays a particular behavior.

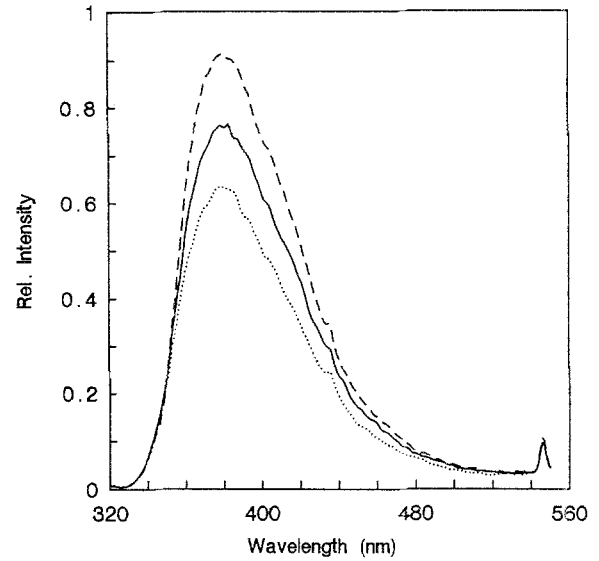


Fig. 13. Fluorescence spectra of 12COB in the  $S_A$  phase (cell thickness  $\approx 20 \mu\text{m}$ ,  $T = 85^\circ\text{C}$ ):  $\vec{E} = 0$  (—); AC  $f = 80 \text{ Hz}$ ,  $120 V_{eff}$  (- - -); AC  $f = 15 \text{ kHz}$ ,  $120 V_{eff}$  (.....).

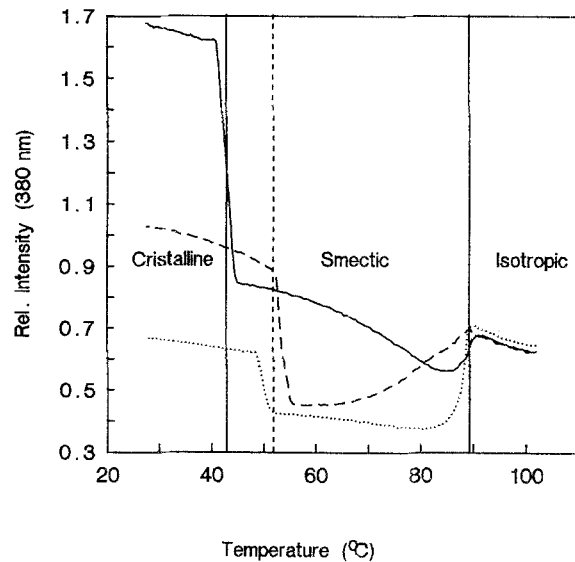


Fig. 14. Fluorescence intensity ( $\lambda_{EM} = 380 \text{ nm}$ ) of 12COB versus the temperature (cell thickness  $\approx 20 \mu\text{m}$ ):  $\vec{E} = 0$  (—); AC  $f = 80 \text{ Hz}$ ,  $120 V_{eff}$  (- - -); AC  $f = 15 \text{ kHz}$ ,  $120 V_{eff}$  (.....).

Up to  $10^\circ\text{C}$  below  $T_{IS}$  the transmittance is very low (20%). With decreasing temperature the turbulent flow decreases, resulting in larger transmittance value. Finally, a homeotropic orientation is achieved which displays a high transmittance value (93% at  $55^\circ\text{C}$ ).

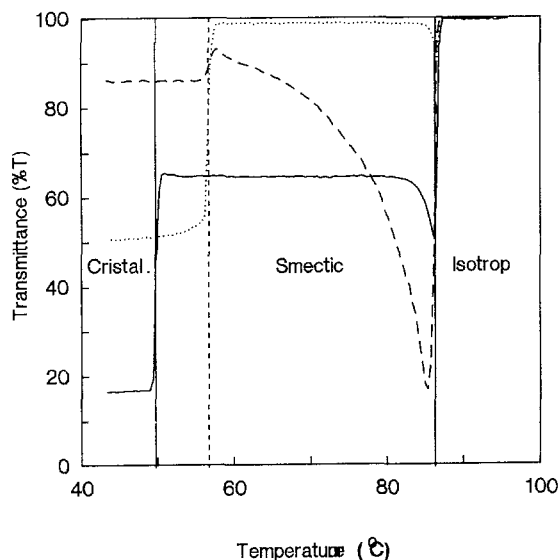


Fig. 15. Transmittance ( $\lambda = 700$  nm) of  $\downarrow$ 2COB as a function of the temperature (cell thickness  $\approx 20$   $\mu\text{m}$ ):  $E = 0$  (—); AC  $f = 80$  Hz,  $120 V_{\text{eff}}$  (---); AC  $f = 15$  kHz,  $120 V_{\text{eff}}$  (.....).

## CONCLUSIONS

By means of the fluorescence technique, information about the characteristic properties of the Frederickz transition in the liquid crystalline phases can be obtained. Response times in the order of milliseconds are accurately determined. Furthermore, information about the reversibility of the deformation in the nematic and the smectic A phase is acquired. The fluorescence data are compared with the results from the turbidity experiments, and a good correlation between the two techniques is observed. The experimental findings agree with the general principles of the Frederickz transition and the dynamic scattering, based on electrooptical measurements.

## ACKNOWLEDGMENTS

The financial support of ICI, through a J.R.S. of the ministry of "Wetenschapsbeleid," through I.U.A.P.3 and a concerted action, as well as that of the Belgian National Science Foundation, is gratefully acknowl-

edged. Dr. N. Boens is thanked for the development of the deconvolution program.

## REFERENCES

1. H. Kelker and R. Hatz (1980) in *Handbook of Liquid Crystals*, Verlag Chemie, Weinheim, pp. 174–207.
2. V. Frederickz and V. Zolina (1933) *Trans. Faraday. Soc.* **29**, 919–930.
3. R. Steinsträßer and L. Pohl (1973) *Angew. Chem.* **85**, 706–718.
4. D. Coates, W. A. Crossland, J. H. Morrissy, and B. Needham (1978) *J. Phys. D Appl. Phys.* **11**, 2025–2034.
5. M. Hareng, S. Le Berre, and L. Thirant (1974) *Appl. Phys. Lett.* **25**, 683–697.
6. H. Finkelmann, U. Kiechle, and G. Rehage (1983) *Mol. Cryst. Liq. Cryst.* **94**, 343–358.
7. H. Finkelmann, D. Naegelé, and H. Ringsdorf (1979) *Makromol. Chem.* **180**, 803–806.
8. R. Simon and H. J. Coles (1984) *Mol. Cryst. Liq. Cryst.* (letters) **102**, 43–48.
9. R. Simon and H. J. Coles (1984) *Mol. Cryst. Liq. Cryst.* (letters) **102**, 75–80.
10. H. Ringsdorf and R. Zentel (1982) *Makromol. Chem.* **183**, 1245–1256.
11. D. Markovitsi and J. P. Ide (1986) *J. Chim. Phys.* **83**, 97–102.
12. C. David and C. Bayens-Volant D. (1984) *Mol. Cryst. Liq. Cryst.* **106**, 45–65.
13. C. David and D. Bayens-Volant (1985) *Mol. Cryst. Liq. Cryst.* **116**, 217–243.
14. C. David and D. Bayens-Volant (1980), *Mol. Cryst. Liq. Cryst.* **59**, 181–196.
15. R. Subramanian, L. K. Patterson, and H. Levanon (1982) *Chem. Phys. Lett.* **93**, 578–581.
16. N. Tamai, I. Yamazaki, H. Masuhara, and N. Mataga (1984), *Chem. Phys.* **106**, 485–488.
17. N. Tamai, I. Yamazaki, H. Masuhara, and N. Mataga (1984), *Springer Ser. Chem. Phys.* **38**, 355–361.
18. T. Ikeda, S. Kurihara, N and S. Tazuke (1990) *Liq. Cryst.* **7**, 749–752.
19. D. Markovitsi, M. Mouallem, F. Rigaud, and J. Malthete (1987) *Chem. Phys. Lett.* **135**, 236–242.
20. D. Markovitsi, I. Lécuyer, B. Clergeot, C. Jallabert, H. Strzelecka, and M. Veber (1989) *Liq. Cryst.* **6**, 83–92.
21. Y. Shimoyama, M. Shiotani, and J. Sohma (1977) *Jap. J. Appl. Phys.* **16**, 1437–1443.
22. E. Constant, J. P. Parneix, and A. Chapoton (1975) *J. Phys. (Paris)* **38**, 1143–1149.
23. C. Druon and J. M. Wacrenier (1977) *J. Phys. (Paris)* **38**, 47–50.
24. (a) M. Van De Zegel, N. Boens, D. Daems, and F. C. De Schryver (1986) *Chem. Phys.* **101**, 311–335. (b) M. Van De Zegel, N. Boens, and F. C. De Schryver (1984) *Chem. Phys. Lett.* **111**, 340–346.
25. D. Marquardt (1963) *J. Soc. Indust. Appl. Mat.* **2**, 431.
26. W. Rettig (1986) *Angew. Chem.* **98**, 969–986.
27. A. Klock and W. Rettig (1988) *XII UIPAC Symposium on Photochemistry Bologna*, PK 16–17.
28. J. Hofkens, M. Van Damme, F. C. De Schryver, A. Klock, and W. Rettig, in preparation.